

PAPER

Phase transition and electrical properties of aggregations of ethoxylated phytosterol surfactants by dielectric spectroscopy

To cite this article: Xue Li and Kongshuang Zhao 2018 *J. Phys.: Condens. Matter* **30** 505402

View the [article online](#) for updates and enhancements.



IOP | ebooks™

Bringing you innovative digital publishing with leading voices to create your essential collection of books in STEM research.

Start exploring the [collection](#) - download the first chapter of every title for free.

Phase transition and electrical properties of aggregations of ethoxylated phytosterol surfactants by dielectric spectroscopy

Xue Li and Kongshuang Zhao¹ 

College of Chemistry, Beijing Normal University, Beijing 100875, People's Republic of China

E-mail: zhaoks@bnu.edu.cn

Received 5 July 2018, revised 4 October 2018

Accepted for publication 26 October 2018


Published 22 November 2018



Abstract

The aggregation behaviors of the bio-friendly nonionic phytosterol ethoxylated (BPS-*n*) surfactants, in water were investigated by dielectric spectroscopy over a frequency range from 40 Hz to 110 MHz. Only the BPS-5 solution system observes dielectric relaxation and we judge this is because due to the difference in the chain length of BPS-*n* surfactants. Then we further analyze the BPS-5 solution system. Interestingly, we found that BPS-5 lamellar aggregations exist two phases before and after 6%–8% BPS-5 concentration by using the dielectric parameters and the phase parameters obtained by fitting dielectric spectrum and the theoretical model respectively. In addition, we concluded that the change of the electrical parameters such as surface conductivity and zeta potential are related to the lamellar phase structure. Besides, lamellar phases formed at a lower concentration are more stable than those at higher concentration by the thermodynamic analysis.

Keywords: phytosterol ethoxylated surfactants, dielectric spectroscopy, phase transition, electrical properties

 Supplementary material for this article is available [online](#)

(Some figures may appear in colour only in the online journal)

1. Introduction

In 1950, Barton proposed and clarified the stereoscopic structure of steroids [1], which led to the theory of organic chemistry. Since then, steroid chemistry has also been developed. Among them, phytosterol ethoxylated surfactants (BPS-*n*, *n* is the oxyethylene (EO) chain length) have provoked interest recently [2] because they are biocompatible, safe, non-toxic and not environmentally harmful, and can be widely applied in cosmetics [3], medicine [4], food industry [5], etc. The unique rigid sterol ring structures of the sterol surfactants exhibit a much stronger segregation tendency compared to the conventional alkyl ethoxylated nonionic surfactants. Thus, sterol surfactants can form rigid ordered aggregations in an aqueous environment easily. The BPS-*n* surfactant can form various aggregations in different solvents [6–10]. Especially,

BPS-*n* surfactants in water form a variety of lyotropic liquid crystals, such as lamellar phase, gel phase, closest packed micellar cubic phase, nematic, and hexagonal phase [10]. The lyotropic liquid crystals are often used to prepare materials as templates, which are typically used for bionic materials [11], drug delivery [12], membrane separation [13], and catalysis [14], especially in the medical field [15–17].

First of all, it is very clear that such a broad applications of BPS-*n* surfactants require relatively stable aggregations, especially in the areas of pharmacokinetics, bio-distribution, and clearance mechanisms for preparation of materials [18]. The stability of aggregations mainly depends on electrical properties of their surface, which govern their aggregation behavior. The reason is that the repulsion and adsorption of charges between ions cause the adsorption layer of ions as a barrier that prevents aggregations from approaching or contacting each other [19]. Zeta potential is often used to characterize the surface electrical properties of aggregations in solution and

¹ Author to whom any correspondence should be addressed.

the stability of colloid systems including surfactant aggregations is studied [20]. The research on BPS-*n* surfactants mainly focuses on constructing different types of aggregations in different solvents [8–10, 21–24] and there are few studies on the double-layer properties of lyotropic liquid crystals formed by BPS-*n* surfactants. Therefore, for their applications in dominating delivering and releasing drugs [25, 26], we want to analyze the electric properties of BPS-*n* aggregations and their aggregation structures.

In addition, a surfactant can form several different lamellar phases in the same solvent due to the disorder and fluidity of the hydrophobic chains of the lamellar phase. There are some reports about the lamellar lyotropic liquid crystals formed by BPS-*n* surfactants [8–10, 23, 27]. Among them, Yue *et al* [27] observed two kinds of lamellar phases in BPS-10/[Bmim]BF₄ system through polarized optical microscopy and small angle x-ray scattering. Similarly, they [8] also found two lamellar phases in BPS-5/glycerol system. Both [Bmim]BF₄ and glycerol as solvents have higher Gordon parameters [28] and similar structural characteristics of polyhydroxyl groups. The driving force of constructing lamellar phase in [Bmim]BF₄ and glycerol is the hydrophobic interactions between steroid rings as well as hydrogen-bonding interactions between EO chains and solvents [8, 27, 29]. Water has the structural characteristics of polyhydroxyl groups like [Bmim]BF₄ and glycerol and has higher Gordon parameters than [Bmim]BF₄ and glycerol [28]. According to the phase diagram of Folmer *et al* [10], BPS-5 aqueous solution within mass fraction of 30% can form lamellar phase from 0 °C to 100 °C. Theoretically, types of BPS-5 aggregations should be more abundant. Therefore, we have the following question: do BPS-5 surfactants only form a kind of lamellar phase within 30%?

Dielectric spectroscopy (DS) is one of the few effective methods to investigate the properties of heterogeneous systems, such as colloid disperse system and biological cell suspension and so on. The structural characteristics and electric/dielectric properties of these systems can be obtained by DS through appropriate models [30]. The studies on the structures and phase transitions of aggregations by DS have been reported recently [31, 32], including ours [33–35]. In the present study, we choose the BPS-*n*/water system as the research object. According to the phase diagram of BPS-*n*/water system given by Folmer *et al* [10], we configured aqueous solutions of four BPS-*n* surfactants within mass fraction of 20% in the experiment to explore the aggregation process and the stability of these aggregations. These BPS-*n* aqueous solutions were measured by DS over the radio frequency range. A unique dielectric relaxation phenomenon was observed just for the BPS-5/water system, while no dielectric relaxations were observed for the BPS-*n* surfactants with longer chains. For further studying the BPS-5/water system, the dielectric data were analyzed to obtain information on phase transitions, thermodynamic parameters and electrical parameters.

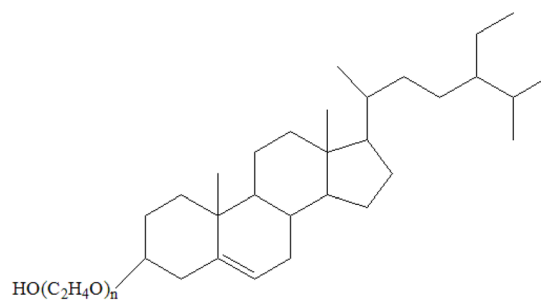


Figure 1. Chemical structure of ethoxylated phytosterol surfactants, $n = 5, 10, 20, 30$.

2. Materials and methods

2.1. Materials and sample preparation

2.1.1. Materials. The nonionic ethoxylated phytosterol surfactants (BPS-*n*, *n* represents oxyethylene chain lengths of 5, 10, 20, and 30) were a generous gift from Nikko Chemicals Shanghai Corporation and used without further purification. The hydrophobic portion of BPS-*n* surfactants consisted of β -sitosterol, campesterol, and stigmasterol in a 2:1:1 weight ratio, and the surfactants contained less than 3 wt% polyoxyethylene as a hydrophilic impurity. The chemical structure of BPS-*n* is shown in figure 1. In addition, doubly distilled water was used for all experiments.

2.1.2. Sample preparation. A series of aqueous solutions according to mass fraction with four different chain lengths BPS-*n* were prepared and the concentrations were from 2 wt% to 20 wt% for involving multiple phase areas. After stirring, centrifugation and ultrasonic, samples were dissolved completely and equilibrated at room temperature for one week waiting for dielectric measurement.

2.2. Dielectric measurement

Dielectric measurements were carried out over a frequency range from 40 Hz to 110 MHz using a 4294A Precision Impedance Analyzer (Agilent Technologies) from 20 °C to 60 °C. The raw experimental data capacitance (C_x) and conductance (G_x) values of samples at different frequencies were measured directly by using the glass cell with the concentric circular Pt electrode. Stray capacitance C_r and cell constant C_l were determined to be 1.437 and 6.150 pF, respectively, by using several standard substances such as air, ethanol and pure water. According to Shwann's method [36], residual inductance L_r (12.16 nH) was determined by a series of different concentrations of KCl solutions. Then, C_x and G_x were corrected applying the following equations [37]:

$$C_s = \frac{C_x (1 + \omega^2 L_r C_x) + L_r G_x^2}{(1 + \omega^2 L_r C_x)^2 + (\omega L_r G_x)^2} - C_r \quad (1)$$

$$G_s = \frac{G_x}{(1 + \omega^2 L_r C_x)^2 + (\omega L_r G_x)^2} \quad (2)$$

Marks x and s represent raw and corrected dates respectively. Then, the corrected data of capacitance C_s and conductance G_s at each frequency were converted to permittivity ε and conductivity κ using the equations:

$$\varepsilon = C_s - C_r/C_l \quad (3)$$

$$\kappa = G_s\varepsilon_0/C_l. \quad (4)$$

ε_0 is the vacuum permittivity, $\varepsilon_0 = 8.8541 \times 10^{-12} \text{ F m}^{-1}$.

2.3. Determination of relaxation

The complex permittivity ε^* of a substance or system under an applied electric field with angular frequency ω can be expressed as

$$\varepsilon^*(\omega) = \varepsilon(\omega) - j\frac{\kappa(\omega)}{\varepsilon_0\omega} = \varepsilon(\omega) - j\varepsilon''(\omega) - \frac{\kappa_1}{\varepsilon_0\omega} \quad (5)$$

where $\varepsilon(\omega)$ and $\varepsilon''(\omega)$ are the frequency-dependent permittivity and dielectric loss of the surfactant solution, i.e. the real and the imaginary part of the complex permittivity, respectively. $\kappa(\omega)$ is the conductivity and κ_1 is low-frequency limit of conductivity, which was read out from the conductivity spectra at low frequency. The dielectric loss was calculated from the conductivity spectra through the equation $\varepsilon'' = \frac{\kappa - \kappa_1}{\varepsilon_0\omega}$. ω is the angular frequency ($\omega = 2\pi f$, where f is the measurement frequency) and $j = \sqrt{-1}$.

Generally, the dielectric spectra over the whole measuring frequency range can be described by the following equation including i ($i = 1, 2, \dots$ indicates the number of dielectric relaxation), the Cole–Cole terms, and one electrode polarization (EP) term $A\omega^{-m}$ (where A and m are adjustable parameters)

$$\varepsilon^* = \varepsilon_h + \sum_i \frac{\Delta\varepsilon_i}{1 + (j\omega\tau_i)^{\beta_i}} + A\omega^{-m} \quad (6)$$

where ε_h is the high-frequency limit of permittivity, $\Delta\varepsilon_i$ and τ_i ($= 1/(2\pi f_{0i})$, f_{0i} is characteristic relaxation frequency) indicate relaxation strength and relaxation time of the i th relaxation, respectively, and β_i ($0 < \beta_i \leq 1$) is the Cole–Cole parameter, indicating the distribution of relaxation times. Parameters ε_1 , ε_h , κ_1 , τ , and β are called dielectric parameters (or relaxation parameters) and can be obtained by fitting the Cole–Cole equation.

It is very clear that two relaxation processes were observed in the measured frequency range in BPS-5 aqueous solution. The middle conductivity κ_m and high conductivity κ_h can be calculated by equations (7) and (8) [38]. An example of the frequency dependence of permittivity of the BPS-5 aqueous solution with mass fraction of 4% at 25 °C was shown in figure 2

$$\kappa_m = ((\varepsilon_1 - \varepsilon_m)2\pi f_1\varepsilon_0) + \kappa_1 \quad (7)$$

$$\kappa_h = ((\varepsilon_m - \varepsilon_h)2\pi f_h\varepsilon_0) + \kappa_m. \quad (8)$$

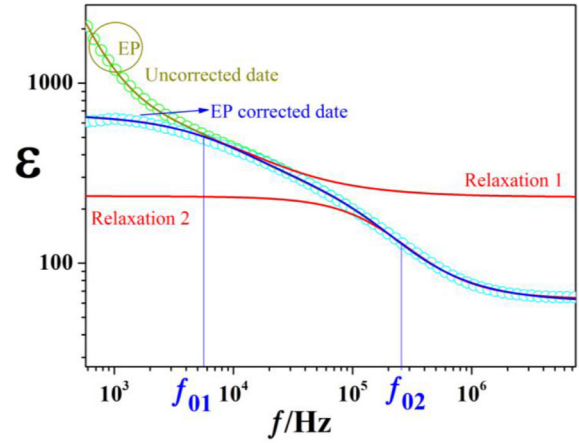


Figure 2. The dielectric spectroscopy for the BPS-5 aqueous solution with mass fraction of wtBPS-5% = 4% at 25 °C. The solid green circles and dark yellow line are the uncorrected raw data and best total fit with EP, respectively. The cyan circles and blue line are the corrected raw data and best total fit without the EP, respectively. Red lines represent the low frequency relaxation (relaxation 1) and high frequency (relaxation 2) relaxation.

2.4. Relevant model and theoretical formulas

Different from the dielectric parameters, the phase parameters can obtain the detailed information about inner structure, such as the permittivity and conductivity of the two phases in suspension, and the volume fraction of the dispersed phase. In our work, the system is that the lamellar phase formed by the BPS-5 surfactant is dispersed in the continuous aqueous phase. Therefore, the Bruggeman's theory [39] and related methods can be applied to the current system. Therefore, in our work, number of lamellar phase particles with permittivity ε_p^* are dispersed to continuous aqueous phase with permittivity ε_a^* in a volume fraction ϕ and complex permittivity ε^* system as illustrated in figure 3. According to Bruggeman's theory [39], by successive infinitesimal additions of particles, the system reaches the final volume fraction ϕ and complex permittivity ε^* , and thus Hanai [40] obtained an integral equation as:

$$\int_0^\phi -\frac{d\phi'}{1-\phi'} = \int_{\varepsilon_a^*}^{\varepsilon^*} \frac{3}{\varepsilon^*(\varepsilon^* - \varepsilon_p^*)} \left[\sum_{k=x,y,z} \frac{1}{\varepsilon^* + (\varepsilon_p^* - \varepsilon^*)L_k} \right]^{-1} d\varepsilon^*. \quad (9)$$

When ellipsoids are oriented such that the k -axis is parallel to the electric field, equation (9) was translated to equation (10) by Boyle [41]

$$1 - \phi = \left(\frac{\varepsilon^* - \varepsilon_p^*}{\varepsilon_a^* - \varepsilon_p^*} \right) \left(\frac{\varepsilon_a^*}{\varepsilon^*} \right)^{L_k}. \quad (10)$$

L_k is called the depolarization factor. For example, $L_k = 1/3$ for spherical particles. For lamellar particles, equation (10) with $L_k = 1$ becomes Hanai's mixture equation [40]:

$$1 - \phi = \left(\frac{\varepsilon^* - \varepsilon_p^*}{\varepsilon_a^* - \varepsilon_p^*} \right) \left(\frac{\varepsilon_a^*}{\varepsilon^*} \right). \quad (11)$$

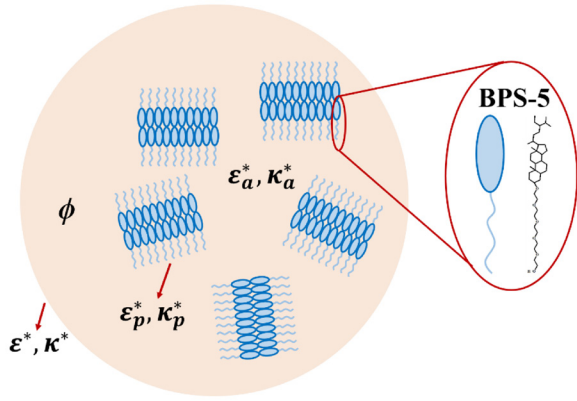


Figure 3. The dielectric model of lamellar liquid crystal phase in suspension.

It should be noted that phase parameters (ε_p , ε_a , κ_p , κ_a , and ϕ) are related to the relaxation parameters (ε_1 , ε_h , κ_1 , κ_h and τ are the low- and high-frequency limits of permittivity, the low- and high-frequency limits of conductivity, and relaxation time, respectively) as follows

$$\frac{\varepsilon_h - \varepsilon_p}{\varepsilon_a - \varepsilon_p} \left(\frac{\varepsilon_a}{\varepsilon_h} \right)^{L_k} = 1 - \phi \quad (12a)$$

$$\varepsilon_1 \left(\frac{3}{\varepsilon_1 - \varepsilon_p} - \frac{1}{\kappa_1} \right) = 3 \left(\frac{\varepsilon_a - \varepsilon_p}{\kappa_a - \kappa_p} + \frac{\varepsilon_p}{\kappa_1 - \kappa_p} \right) - \frac{\varepsilon_a}{\kappa_a} \quad (12b)$$

$$\kappa_1 \left(\frac{3}{\varepsilon_1 - \varepsilon_p} - \frac{1}{\varepsilon_h} \right) = 3 \left(\frac{\kappa_a - \kappa_1}{\varepsilon_a - \varepsilon_p} + \frac{\kappa_1}{\varepsilon_h - \varepsilon_p} \right) - \frac{\kappa_a}{\varepsilon_a} \quad (12c)$$

$$\frac{\kappa_h - \kappa_p}{\kappa_a - \kappa_p} \left(\frac{\kappa_a}{\varepsilon_1} \right)^{L_k} = 1 - \phi. \quad (12d)$$

The phase parameters of lamellar phase can be calculated from the relaxation parameters using equations (12a)–(12d) by a systematic numerical method developed by Hanai *et al* [42]. Besides, ε_a is the permittivity of water, so 80.18, 78.36, 76.58, 73.15, 69.88 and 66.76 is the permittivity of water at 20 °C, 25 °C, 30 °C, 40 °C, 50 °C and 60 °C.

3. Results and discussion

3.1. Dielectric spectrum of BPS-*n*/water systems with different EO chain lengths

Figures 4(a)–(d) show the dielectric spectrum of BPS-*n* aqueous solutions with different mass fraction of wtBPS-*n*. It can be seen from figure 4 that only BPS-5 solution system exhibits relaxations at about 10^5 Hz and the others, i.e. BPS-10, BPS-20, BPS-30 solutions, have no relaxations been observed. It should be noted that in figure 4 the increase of the permittivity with decrease of frequency in the frequency range about 10^3 Hz, circled by a dashed ring, is due to the EP effect, not the phenomenon of the BPS-*n* solution systems. Then, we find an interesting thing from figure 4 by combining Folmer’s phase diagram: only the lamellar aggregations formed by BPS-5 surfactants present the relaxation

phenomenon. Although BPS-10, BPS-20 and BPS-30 surfactants also respectively form different structural aggregations in water phase, like rod micellar (for $n = 10$), cubic phase (for $n = 20, 30$) within the measurement quality score range [10, 43]. The reason can be easily considered as the difference in the surfactants’ EO chain lengths. First of all, according to Israelachvili’s critical packing parameters (CPPs) theory [44], the different EO chain lengths lead to difference. The surfactants with short EO chains have higher CPPs and form lamellar liquid crystal phase of high curvature. In contrast, surfactants with long EO chains have lower CPPs and can form micelle, cubic liquid crystal phase and more of low curvature [10, 24, 45]. Secondly, with EO chain lengths increase, according to the equation $N_{agg} = 4\pi l^3 / V_{core}$ (l is the EO chain length, V_{core} is the volume of hydrophobic steroid of surfactant molecule and four surfactants have the same V_{core} , l and V_{core} can be calculated by Tanford’s formula [46]) [47], the aggregation numbers of aggregation increase and the volume of surfactant molecule become larger. Therefore, with EO chain lengths increase the volume of aggregations become larger [48]. In addition, with EO chain lengths increase, the hydrogen bond interactions between hydrophilic EO chains increase resulting in aggregations gathering more tightly. To sum up, the volumes of micelle and cubic liquid crystal phase, packed densely and formed by BPS-*n* surfactants with larger EO chain length, is larger. In the range of measured frequency (40–110 MHz), the orientation of larger aggregations of micelle and cubic phase packed densely is difficult, and the relaxations of micelle and cubic phase may occur at the low radio frequency or audio segment outside the range of measurement as shown in some works [31, 49, 50].

3.2. Transformations of lamellar phase

3.2.1. Permittivity spectra at of varying mass fractions and temperatures.

Figures 5(a) and (b) are the three-dimensional representations of dielectric spectra for BPS-5 aqueous solutions with different mass fraction at different temperature. To examine the dielectric spectra in detail, one typical fitting example at 25 °C with the mass fraction of wtBPS-5% = 4% is shown as figure 2. There are low and high dielectric relaxations locating at frequencies around 10^3 Hz and 10^5 Hz caused by ionic polarization and interface polarization, respectively. Because of BPS-5 surfactants’ impurities [24], pH of BPS-5 solutions is characterized below 7. Therefore, the EO chains of BPS-5 can absorb more H^+ . H^+ moves along the EO chains under an applied electric field, resulting in the so-called counterion polarization at lower frequency (see figure 5). On the other hand, the ions move by the electric field and accumulate on the surface of the lamellar aggregation formed by BPS-5, leading to a dielectric relaxation caused by interfacial polarization. This relaxation appears at higher frequency as can be seen in the inset of the figure 5. From figures 5(a) and (c), it is noteworthy that when the mass fraction is about 6%–8%, the permittivity of the system changes suddenly as indicated by the inset of figure 5(a), implying that the phase transformation occurs. In addition, the permittivity

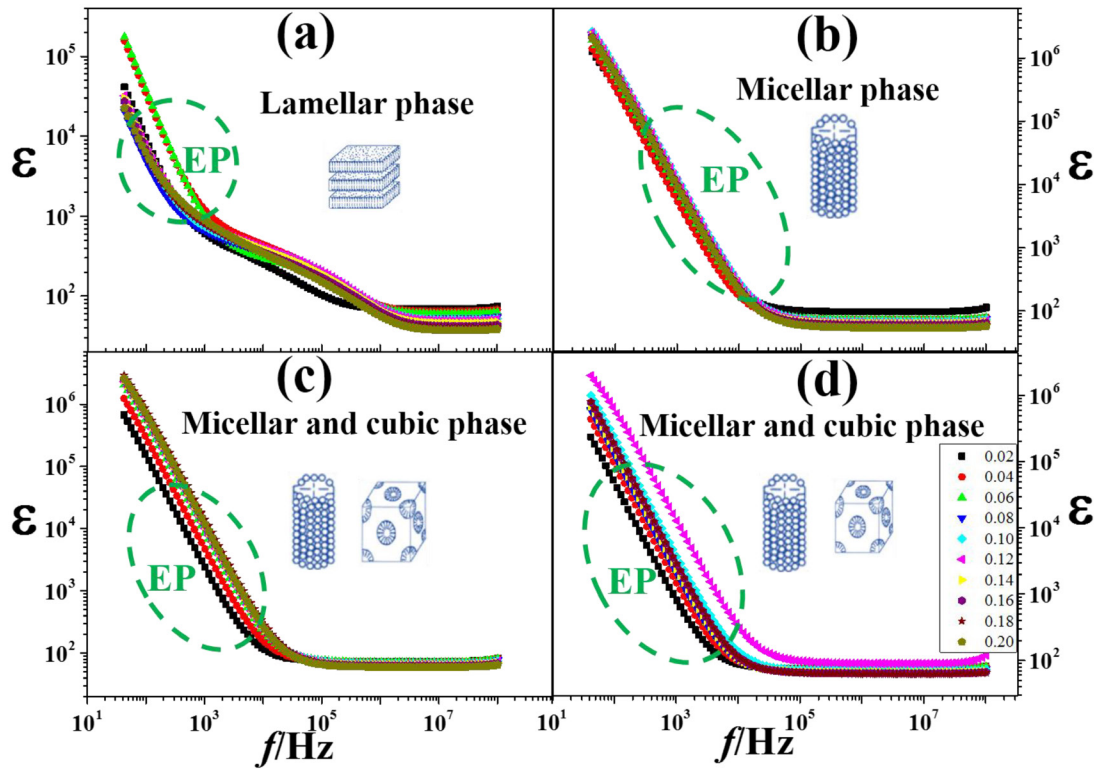


Figure 4. The dielectric spectroscopy for the BPS-5 (a), BPS-10 (b), BPS-20 (c) and BPS-30 (d) aqueous solutions with mass fraction of BPS-n from 2% to 20% at 25 °C; the insets represent different surfactants forming different aggregates within the measured concentration range.

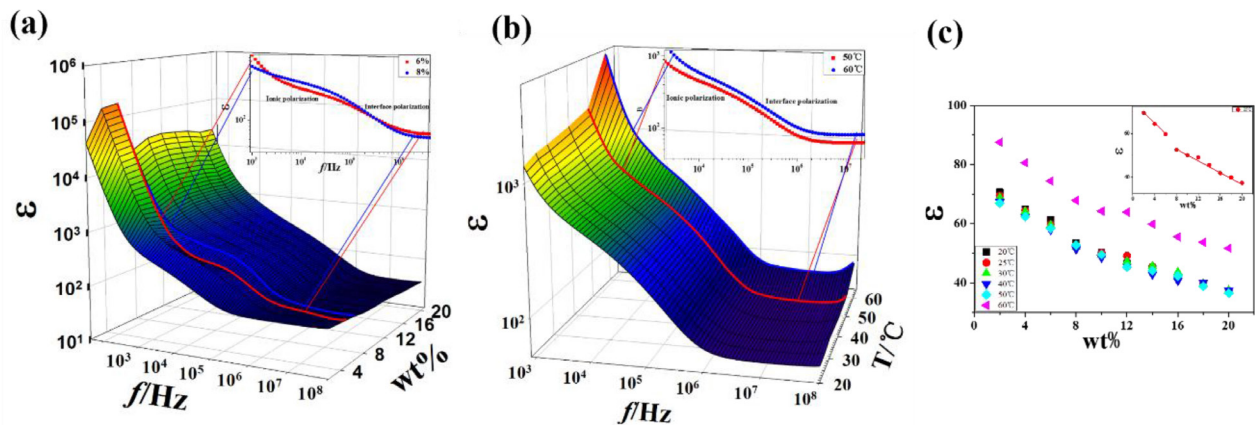


Figure 5. Three-dimensional representations of dielectric spectra for (a) aqueous solution with different mass fraction of BPS-5 at 25 °C and (b) for aqueous solution with mass fraction of wtBPS-5% = 4% at different temperature, the insets show the change of permittivity above and below the phase transformation. (c) Permittivity for aqueous solution with different mass fraction BPS-5 at different temperature, the inset show the dielectric spectra at 25 °C.

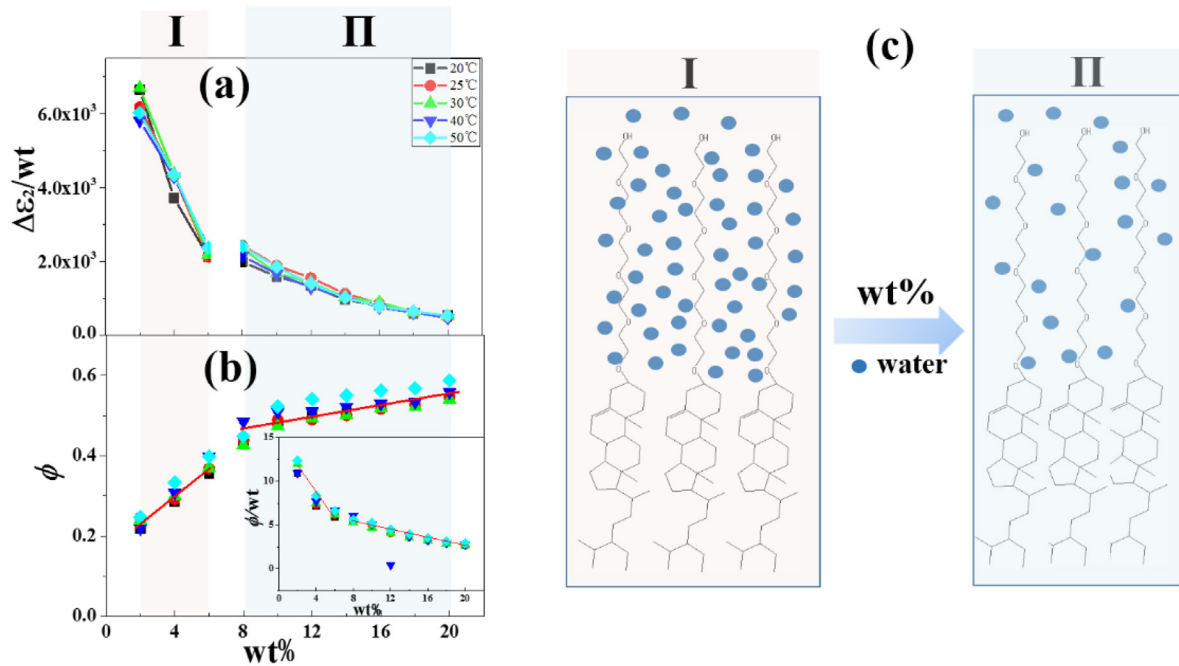
also show a great difference at about 60 °C compared with in other temperatures for the same mass fraction as shown in the figures 5(b) and (c). This may show that when the system reaches a certain temperature, lamellar aggregate structure also changes. In other words, both of the concentration and the temperature of the BPS-5 solutions effect lamellar structure.

3.2.2. Determination of transformations of lamellar phase. To obtain the information on the phase transition and the microscopic structure of the lamellar phase, we focus on the dielectric spectroscopy of BPS-5 solutions when their mass

fraction changes from 2% to 20%. Figure 2 shows one typical fitting result using equation (6) for this system, the details of the fitting procedures have been introduced in section 2.3. By the fitting, corresponding relaxation parameters of BPS-5 system such as relaxation time τ and dielectric increment (relaxation strength) $\Delta\epsilon$, were obtained and are partly listed in table 1. The concentration dependence dielectric increment $\Delta\epsilon$, on the mass fraction of BPS-5 for different temperatures is shown in figure 6(a). Besides, in order to further determine the phase transition of the lamellar phase, we analyzed the relaxation spectra at higher frequency theoretically by using

Table 1. Relaxation parameters of aqueous solution with different mass fraction of BPS-5 at varying temperatures.

Sample	$\Delta\epsilon_1$	$\Delta\epsilon_2$	$\Delta\kappa_1$ (10^5 S m^{-1})	$\Delta\kappa_2$ (10^4 S m^{-1})	τ_1 (10^6 s)	τ_2 (10^7 s)
BPS-5-2%-25 °C	343.86 ± 3.24	123.49 ± 2.18	6.10 ± 0.12	2.38 ± 0.09	49.93 ± 0.27	45.91 ± 0.32
BPS-5-4%-2 °C	418.92 ± 4.28	172.66 ± 1.43	20.80 ± 0.22	13.28 ± 0.12	17.83 ± 0.28	11.51 ± 0.17
BPS-5-6%-25 °C	256.68 ± 1.53	127.47 ± 1.74	14.03 ± 0.18	12.43 ± 0.15	16.20 ± 0.12	9.08 ± 0.12
BPS-5-8%-25 °C	354.82 ± 4.42	194.43 ± 3.15	11.30 ± 0.20	14.94 ± 0.13	27.79 ± 0.23	11.53 ± 0.11
BPS-5-10%-25 °C	380.05 ± 2.48	189.00 ± 2.45	14.24 ± 0.17	20.09 ± 0.19	23.64 ± 0.20	8.33 ± 0.13
BPS-5-12%-25 °C	412.29 ± 4.77	186.83 ± 4.75	17.27 ± 0.14	20.63 ± 0.17	21.13 ± 0.22	8.02 ± 0.18
BPS-5-14%-25 °C	416.64 ± 2.92	158.30 ± 2.91	20.56 ± 0.19	19.22 ± 0.14	17.94 ± 0.19	7.29 ± 0.10
BPS-5-16%-25 °C	411.48 ± 1.95	138.37 ± 3.83	18.62 ± 0.21	18.04 ± 0.22	19.57 ± 0.18	6.79 ± 0.13
BPS-5-18%-25 °C	511.14 ± 3.24	113.26 ± 1.48	14.92 ± 0.15	12.85 ± 0.12	30.34 ± 0.27	7.81 ± 0.11
BPS-5-20%-25 °C	524.92 ± 4.67	97.44 ± 2.56	16.53 ± 0.17	11.66 ± 0.16	28.12 ± 0.24	7.40 ± 0.14
BPS-5-2%-30 °C	309.14 ± 2.37	133.78 ± 1.98	6.58 ± 0.15	2.41 ± 0.13	41.57 ± 0.29	49.21 ± 0.32
BPS-5-4%-30 °C	409.56 ± 3.51	175.09 ± 4.71	20.27 ± 0.24	14.66 ± 0.18	17.89 ± 0.15	10.58 ± 0.16
BPS-5-6%-30 °C	277.05 ± 1.78	131.23 ± 3.28	12.73 ± 0.19	13.18 ± 0.15	19.27 ± 0.14	8.82 ± 0.13
BPS-5-8%-30 °C	354.98 ± 2.49	187.75 ± 3.57	11.80 ± 0.17	15.17 ± 0.12	26.64 ± 0.20	10.96 ± 0.17
BPS-5-10%-30 °C	394.15 ± 3.86	167.97 ± 1.29	19.53 ± 0.20	21.89 ± 0.21	17.87 ± 0.18	6.79 ± 0.12
BPS-5-12%-30 °C	432.11 ± 2.34	171.42 ± 2.35	21.30 ± 0.18	22.21 ± 0.25	17.97 ± 0.16	6.83 ± 0.14
BPS-5-14%-30 °C	461.88 ± 4.06	145.73 ± 3.07	23.33 ± 0.24	18.80 ± 0.19	17.53 ± 0.13	6.86 ± 0.17
BPS-5-16%-30 °C	436.62 ± 3.14	144.13 ± 2.26	23.52 ± 0.23	20.98 ± 0.22	16.44 ± 0.12	6.08 ± 0.11
BPS-5-18%-30 °C	559.93 ± 3.25	113.91 ± 4.24	16.63 ± 0.12	14.20 ± 0.15	29.81 ± 0.25	7.10 ± 0.15
BPS-5-20%-30 °C	545.56 ± 4.53	103.65 ± 1.90	16.34 ± 0.18	11.99 ± 0.24	29.56 ± 0.21	7.66 ± 0.10

**Figure 6.** (a) Dielectric increments $\Delta\epsilon$ and (b) volume fraction ϕ of lamellar aggregation with different mass fraction of BPS-5, the inset shows the dependence of ϕ/wt with different mass fraction of BPS-5; (c) lamellar phase structure above and below the phase transformation.

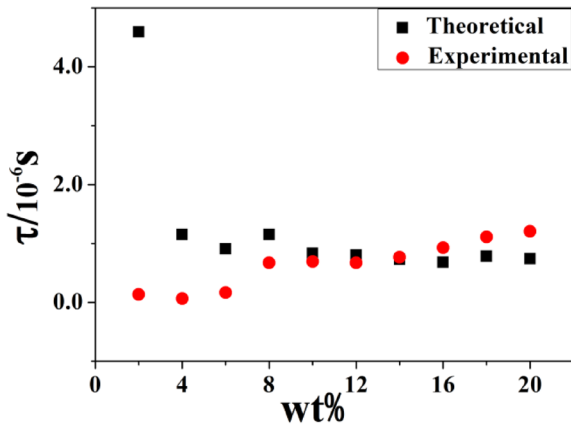
these relaxation parameters coupled with the relevant model mentioned above. The phase parameters, such as permittivity ϵ and volume fraction ϕ , are summarized in table 2. The concentration dependence of the volume fraction ϕ of lamellar aggregations is shown as figure 6(b).

From figure 6(a), it can be seen that within the studied concentration the dielectric increments $\Delta\epsilon$ are divided into two

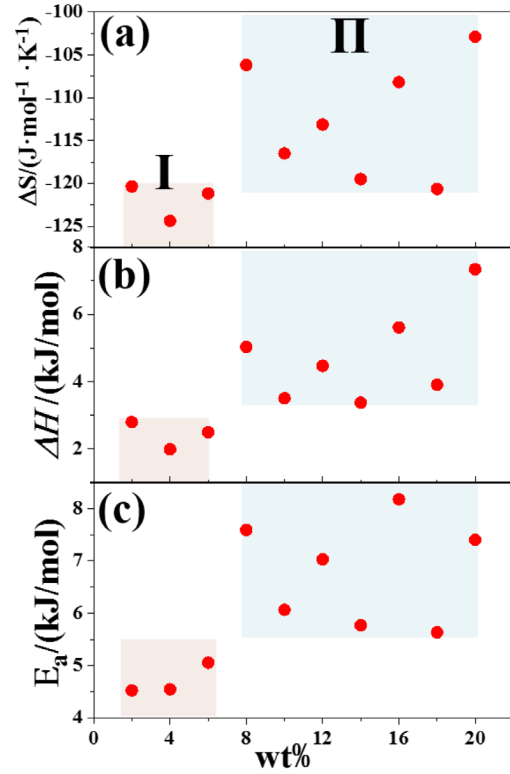
phases of I and II by Wt . $\Delta\epsilon$ declined sharply as Wt increased when mass fraction of BPS-5 closes to 6% and the decline become relatively stable when it above 8%. The change of volume fraction ϕ as Wt is similar to $\Delta\epsilon$. Whatever the case, the results of figures 6(a) and (b) suggest that the structure of the lamellar aggregations may change or the transformations of lamellar phase occur around $Wt = 6\% - 8\%$. According

Table 2. Phase parameters of aqueous solution with different mass fraction of BPS-5 at varying temperatures.

Sample	ϕ	ε_i	κ_i (S m ⁻¹)	κ_a (S m ⁻¹)
BPS-5-2%-25 °C	0.2465	41.7423	0.04016	0.00057
BPS-5-4%-25 °C	0.2917	41.3534	0.03752	0.00095
BPS-5-6%-25 °C	0.3683	39.0661	0.01418	0.00093
BPS-5-8%-25 °C	0.4392	33.7872	0.00408	0.00020
BPS-5-10%-25 °C	0.4893	33.5925	0.00422	0.00022
BPS-5-12%-25 °C	0.4900	32.4846	0.00433	0.00023
BPS-5-14%-25 °C	0.5005	29.5569	0.00367	0.00024
BPS-5-16%-25 °C	0.5164	26.0299	0.00300	0.00022
BPS-5-18%-25 °C	0.5269	24.8198	0.00241	0.00021
BPS-5-20%-25 °C	0.5462	23.8344	0.00220	0.00021
BPS-5-2%-30 °C	0.2400	45.3528	0.04027	0.00063
BPS-5-4%-30 °C	0.3002	40.9235	0.03960	0.00099
BPS-5-6%-30 °C	0.3701	39.8823	0.01651	0.00100
BPS-5-8%-30 °C	0.4263	32.1561	0.00496	0.00025
BPS-5-10%-30 °C	0.4740	33.1201	0.00504	0.00029
BPS-5-12%-30 °C	0.4927	30.7312	0.00481	0.00028
BPS-5-14%-30 °C	0.5013	28.9670	0.00406	0.00028
BPS-5-16%-30 °C	0.5181	26.2548	0.00369	0.00026
BPS-5-18%-30 °C	0.5217	24.9855	0.00277	0.00024
BPS-5-20%-30 °C	0.5395	22.3731	0.00251	0.00023

**Figure 7.** M–W relaxation time τ_{MW} and experimental relaxation time τ_{exp} of high frequency of aqueous solution with mass fraction of BPS-5 (wt%) at 25 °C.

to the work of Folmer's group, it is known that the lamellar phase is formed within the measured BPS-5 mass fraction [10]. Therefore, we speculate that two types of lamellar phase aggregations may be formed before and after wtBPS-5 = 6%–8%. Besides, as shown in figure 6(b), with the concentration of BPS-5 surfactants increases, the increase of ϕ indicates that number of lamellar phase increase. However, ϕ/wt decreases which implies the decrease of the volume of lamellar phase with the concentration of BPS-5 surfactants increases. The reason is that with the increase of concentration, the interaction between the EO chains increases and the water molecules between the EO chains decrease [8], which lead to that aggregations aggregate closely and the lamellar phase volume decreases. In summary, we speculate that

**Figure 8.** The concentration dependence diagram of thermodynamic parameters for interfacial polarization. (a) The entropy change ΔS , (b) the enthalpy change ΔH and (c) the activation energy E_a . (Pink and blue zones represent phase I and phase II, respectively.)

lamellar phase aggregations above and below the phase transformation are shown as figure 6(c).

3.2.3. Relaxation mechanism of high frequency. For the high frequency relaxation caused by interfacial polarization, the theoretical relaxation time τ_{MW} was calculated by using the phase parameters in table 2 and the Maxwell–Wager equation (equation (13)). There is no doubt that the theoretical relaxation time is similar to the actual one obtained experimentally as shown in figure 7. This verified the mechanism of interface polarization of high-frequency relaxation. This result also shows that the model proposed above to analyze our systems is reasonable for dealing with the lamellar phase system and the result is credible

$$\tau_{MW} = \frac{2\varepsilon_a + \varepsilon_p + \phi(\varepsilon_a - \varepsilon_p)}{2\kappa_a + \kappa_p + \phi(\kappa_a - \kappa_p)} \varepsilon_0. \quad (13)$$

3.3. Thermodynamic analysis of relaxation processes of high frequency

Temperature can change the thermodynamic motion of molecules and the viscosity of solvents, which can further affect the hydrogen bonding between surfactants and solvents. Moreover, the temperature dependence of dielectric spectra can provide thermodynamic function for assessing relaxation processes, and then various interactions of the BPS-5 aqueous system can be discussed. The relationship between

temperature, relaxation time and thermodynamic function follows the Arrhenius equation (equation (14)) and the Eyring equation (equation (15)) [51, 52]:

$$\ln \tau = A + \frac{E_a}{k_B T} \quad (14)$$

$$\ln \tau T = \ln \left(\frac{h}{k_B} \right) - \frac{\Delta S}{R} + \frac{\Delta H}{RT} \quad (15)$$

where h is Planck's constant, R and k_B represent the gas constant and Boltzmann's constant. Thermodynamic parameters (E_a , ΔH and ΔS , represent the activation energy, enthalpy change and entropy change of relaxation processes, respectively) are all relevant to the interaction between water and BPS-5 surfactants.

Further, according to the Arrhenius equation and the Eyring equation, $\ln \tau$ was plotted with $1/T$ by using high-frequency relaxation time in table 1 (and online supplement 1 (stacks.iop.org/JPhysCM/30/505402/mmedia)), and the activation energy E_a for the relaxation process caused by interface polarization can be obtained from the slope. Similarly, from the slope and intercept of $\ln \tau T - 1/T$ curve, the enthalpy ΔH and the entropy ΔS of the same relaxation process can also be obtained. The concentration dependences of thermodynamic parameters for interfacial polarization are shown in figure 8.

From figure 8, the thermodynamic parameters were divided into two phases (phase I and phase II, marked with different colours) at about 6%–8% of BPS-5. Two phases indicates that two kinds of aggregations with different structures forms before and after the concentration point of 6%–8%, respectively, as discussed in section 3.2.2. The values of E_a , ΔH and ΔS in the two phases are significantly different from each other. Both of E_a and ΔH in the phase II are larger than that in phase I (see figures 8(b) and (c)). The difference in E_a indicates that the ionic movement in the phase II is more difficult than that in the phase I. This may be related to the smaller distance between the hydrophilic EO chains in the phase II where the lamellar phases are packed closely at higher concentration [8, 24]. Moreover, the difference of ΔH for the two aggregations indicates that lamellar phase formed in the phase I is more stable than in the phase II. Besides, ΔS of the phase II is less than that of the phase I. This also validated the predictions that the lamellar phases formed in the phase II are packed closely.

3.4. Electrical properties on BPS-5 surfactants aggregation surface

As described in the introduction, the electrical properties of aggregations determine their stability in solution and such their applications. The electro-dynamic formula of the colloidal interface to calculate the electrical parameters of the lamellar phase surface were calculated using following electro-dynamic formula (equations (16)–(18)) and dielectric parameters in table 2. Equation (16) [53] gives the relationship between the dielectric increment and the electrical properties of the aggregation surface

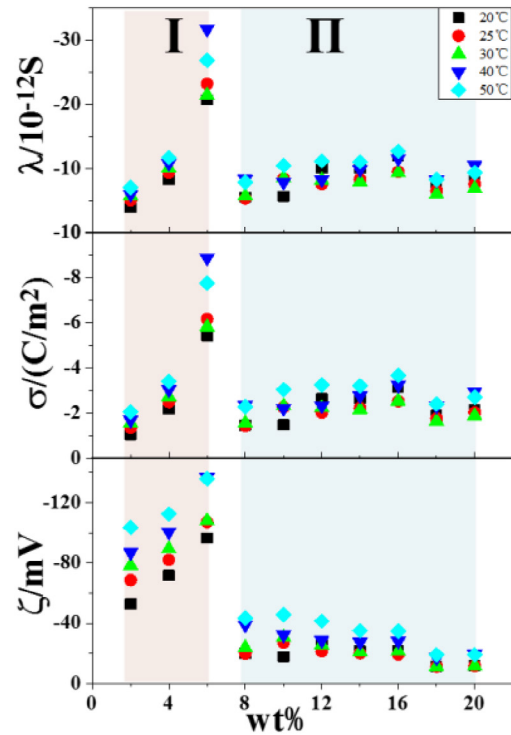


Figure 9. Concentrations dependence of surface electrical parameters of lamellar phase in BPS-5 aqueous system.

$$\Delta \varepsilon_2 = 9\phi \frac{(\varepsilon_p \kappa_a - \varepsilon_a (\kappa_p + 2\lambda/\alpha))^2 (1 - \phi)}{[(1 - \phi) \varepsilon_p + (2 - \phi) \varepsilon_a] [(1 - \phi) (\kappa_p + 2\lambda/\alpha) + (2 + \phi) \kappa_a]^2} \quad (16)$$

where $\Delta \varepsilon_2 = \varepsilon_m - \varepsilon_h$ (ε_m and ε_h are the middle- and high-frequency limits of permittivity respectively and given in the table 1) is the high-frequency relaxation strength due to interfacial polarization, the meanings of ε_a , ε_p , κ_a , κ_p and ϕ have been given in the previous model; λ is the surface conductivity of the lamellar aggregations, α is the radius of the lamellar aggregations. The surface conductivity σ of the lamellar aggregations was calculated through equation (17) and λ that obtained from the dielectric parameters and phase parameters using following equation (16)

$$\sigma = \frac{\lambda}{z^2 \mu} \quad (17)$$

where z is the valence of free charge and μ is the mobility of counterion H^+ . The relationship between the zeta potential ζ and the surface charge density σ is as shown by following equation (18) [54]:

$$\sigma = \frac{4C_e e}{\chi} \sinh \left(\frac{e\zeta}{2kT} \right) \quad (18)$$

where e is the quantity of elementary free charge, k is the Boltzmann constant, T is the absolute temperature, C_e is the concentration of electrolyte solution, χ is reciprocal to the electrical double layer thickness, which is given in the formula $\chi = \sqrt{\varepsilon_a \varepsilon_0 D_{H^+} / \kappa_1}$ (κ_1 is the low-frequency conductivity of

the solution, D_{H^+} is the diffusion coefficient of the H^+ and is estimated to be $9.311 \times 10^{-9} \text{ m}^2 \text{ s}^{-1}$ [55] [56].

As seen from figure 9, in the range of 20 °C–50 °C, the change trend of the electrical parameters with concentration increase is similar and these parameters are also divided into two phases at about 6%–8% of BPS-5. Since the BPS-5 surfactant mainly contains sterol and EO chains, in which the EO chain is slightly negatively charged and the sterol is slightly positively charged, the BPS-5 surfactant is relatively neutral [57]. The data of zeta potential ζ shows that all aggregations have a slightly negative zeta potential since the zeta potential arises from the chemical moieties presented at the lamellar phase surface, which are EO chains. Zana *et al* [58] studied the aggregation number of a series of surfactants and found that the number of aggregations increase with concentration increasing by fluorescence probing method. For the phase I at lower concentrations, with the concentration increases the number of lamellar aggregations increases. The surface charge density σ and ζ increase as a macroscopic phenomenon. On this basis, the ions accumulate on the interfaces as polarized charges and lead to the transferring of more counterions in diffusion layer to keep charges balance under external applied electric field. Hence, the surface conductivity λ increases with the concentration increases. As concentration of the BPS-5 surfactant increases, we conclude that the aggregation of BPS-5 surfactant, negative charge on the surface of the lamellar phase and H^+ absorbed may achieve a relatively stable state. Therefore, for the phase II at higher concentrations, with the concentration increases, the values of σ and ζ do not change substantially. Hence, λ remains substantially unchanged.

The zeta potential of nonionic surfactants containing EO chains aqueous solution (e.g. Tween) is about -40 mV whose absolute value is smaller than our zeta potential [59–61]. This is because of the higher concentration of BPS-5 surfactant as well as its different molecular structure. Besides, the Zeta potential is an important electrical parameter for measuring the stability of the aggregations [20] and our experimental results show that the zeta potential of the phase I is higher than that of the phase II. Therefore, we think the stability of the lamellar phase formed in the low concentration of BPS-5 surfactant is better than that in the high concentration. The electrical parameters calculated by dielectric spectroscopy, especially zeta potential, have certain reference for drug delivery [61].

4. Conclusion

In the present work, aggregation of BPS-*n* surfactant, especially BPS-5, aqueous solutions, was studied systematically by dielectric spectroscopy. The conclusions are divided into the following four parts:

Firstly, two dielectric relaxations were observed over the 40 Hz–110 MHz frequency range just for BPS-5 aqueous system, while no relaxation was observed for the BPS-10, BPS-20 and BPS-30 aqueous systems. We judge this is because of the difference in the EO chain lengths of BPS-*n* surfactants. The

increase of the EO chain length causes that the volume of surfactant aggregations become bigger and aggregations pack closely. The dielectric relaxation of bigger aggregations may exist beyond the experimental frequency range.

Secondly, we further analyze the lamellar phase aggregations in the BPS-5 aqueous system. The two relaxations were identified as ionic polarization for lower frequency and interfacial polarization for higher frequency, respectively. Through obtained dielectric parameters and phase parameters, we find that the lamellar aggregations exist two forms before and after mass fraction of 6%–8%, i.e. phase changes occurs with BPS-5 concentration changes.

Thirdly, the interactions between different lamellar phases are different and the lamellar phase formed at lower concentration of BPS-5 is more stable than that at higher concentration by calculating thermodynamic parameters.

Lastly, we analyze the electric parameters of the lamellar aggregation surface and conclude that the changes of the electric parameters are related to the lamellar aggregation structure. Zeta potential of lamellar aggregation at lower concentration is higher than that at higher concentration and this also proves that the stability of the lamellar phase formed at lower concentration is better than that at higher concentration.

Acknowledgments

This work was supported by the National Natural Science Foundation of China (Grant No. 21173025, 21473012, and 21673002).

ORCID iDs

Kongshuang Zhao  orcid.org/0000-0001-5863-2017

References

- [1] Barton D 1950 The conformation of the steroid nucleus *Experientia* **6** 316–20
- [2] Fernandes P and Cabral J M 2007 Phytosterols: applications and recovery methods *Bioresour. Technol.* **98** 2335–50
- [3] Lundmark L D 1978 Phytosterols for cosmetics *Household Pers. Prod. Ind.* **15** 64–5
- [4] Saleem M 2009 Lupeol, a novel anti-inflammatory and anti-cancer dietary triterpene *Cancer Lett.* **285** 109–15
- [5] Moreau R A, Whitaker B D and Hicks K B 2002 Phytosterols, phytostanols, and their conjugates in foods: structural diversity, quantitative analysis, and health-promoting uses *Prog. Lipid Res.* **41** 457–500
- [6] Müller-Goymann C 1984 Liquid crystals in emulsions, creams, and gels containing ethoxylated sterols as surfactant *Pharm. Res.* **1** 154–8
- [7] van Hal D A *et al* 1996 Preparation and characterization of nonionic surfactant vesicles *J. Colloid Interface Sci.* **178** 263–73
- [8] Qian Z *et al* 2015 Unique lamellar lyotropic liquid crystal phases of nonionic phytosterol ethoxylates in glycerol *Rsc Adv.* **5** 101393–400
- [9] Yi S *et al* 2017 ‘Rigid’ luminescent soft materials: europium-containing lyotropic liquid crystals based on

- polyoxyethylene phytosterols and ionic liquids *J. Phys. Chem. B* **121** 9302–10
- [10] Folmer B M *et al* 1999 The physicochemical behavior of phytosterol ethoxylates *J. Colloid Interface Sci.* **213** 112–20
- [11] Keplinger C and Suo Z 2013 Stretchable, transparent, ionic conductors *Science* **341** 984
- [12] Milak S and Zimmer A 2015 Glycerol monooleate liquid crystalline phases used in drug delivery systems *Int. J. Pharm.* **478** 569–87
- [13] Bara J E *et al* 2010 Room-temperature ionic liquids and composite materials: platform technologies for CO₂ capture *Acc. Chem. Res.* **43** 152–9
- [14] Gin D L *et al* 2006 Recent advances in the design of polymerizable lyotropic liquid-crystal assemblies for heterogeneous catalysis and selective separations *Adv. Funct. Mater.* **16** 865–78
- [15] Zabara A and Mezzenga R 2014 Controlling molecular transport and sustained drug release in lipid-based liquid crystalline mesophases *J. Control Rel.* **188** 31–43
- [16] Guo C *et al* 2010 Lyotropic liquid crystal systems in drug delivery *Drug Discov. Today* **15** 1032–40
- [17] Huang Y and Gui S 2018 Factors affecting the structure of lyotropic liquid crystals and the correlation between structure and drug diffusion *RSC Adv.* **8** 6978–87
- [18] Libster D *et al* 2009 Soft matter dispersions with ordered inner structures, stabilized by ethoxylated phytosterols *Colloids Surf. B* **74** 202–15
- [19] Rosen M J and Kunjappu J T 2012 *Surfactants and Interfacial Phenomena* (New York: Wiley)
- [20] Hunter R J, Ottewill R H and Rowell R L 2013 *Zeta Potential in Colloid Science* (New York: Academic)
- [21] Sakai H *et al* 2009 Phytosterol ethoxylates in room-temperature ionic liquids: excellent interfacial properties and gel formation *Langmuir* **25** 2601–3
- [22] Sakai K *et al* 2011 Adsorption of phytosterol ethoxylates on silica in an aprotic room-temperature ionic liquid *Langmuir* **27** 3244–8
- [23] Yue X *et al* 2013 Lyotropic liquid crystalline phases of a phytosterol ethoxylate in amide solvents *Langmuir* **29** 11013–21
- [24] Misono T *et al* 2015 Ternary phase behavior of phytosterol ethoxylate, water, and imidazolium-based ionic liquid systems—lyotropic liquid crystal formation over a wide range of compositions *Colloids Surf. A* **472** 117–23
- [25] Angius R *et al* 2006 Molecular recognition and controlled release in drug delivery systems based on nanostructured lipid surfactants *J. Phys.: Condens. Matter* **18** S2203–20
- [26] Makai M *et al* 2003 Structure and drug release of lamellar liquid crystals containing glycerol *Int. J. Pharm.* **256** 95–107
- [27] Yue X *et al* 2011 Lyotropic liquid crystalline phases formed by phytosterol ethoxylates in room-temperature ionic liquids *Colloids Surf. A* **392** 225–32
- [28] Greaves T L and Drummond C J 2008 Ionic liquids as amphiphile self-assembly media *Chem. Soc. Rev.* **37** 1709–26
- [29] Auvray X *et al* 1991 Structure of lyotropic phases formed by sodium dodecyl sulfate in polar solvents *Langmuir* **7** 2385–93
- [30] Asami K 2002 Characterization of heterogeneous systems by dielectric spectroscopy *Prog. Polym. Sci.* **27** 1617–59
- [31] He R and Craig D Q M 1998 Identification of thermotropic phase transitions of glyceryl monoolein-water systems by low frequency dielectric spectroscopy *Int. J. Pharm.* **169** 131–41
- [32] Velayutham T S *et al* 2016 Molecular dynamics of anhydrous glycolipid self-assembly in lamellar and hexagonal phases *Phys. Chem. Chem. Phys.* **18** 15182–90
- [33] Lian Y and Zhao K 2011 Study of micelles and microemulsions formed in a hydrophobic ionic liquid by a dielectric spectroscopy method. I. Interaction and percolation *Soft Matter* **7** 8828–37
- [34] Fan X and Zhao K 2014 Aggregation behavior and electrical properties of amphiphilic pyrrole-tailed ionic liquids in water, from the viewpoint of dielectric relaxation spectroscopy *Soft Matter* **10** 3259–70
- [35] Wang S and Zhao K 2016 Dielectric analysis for the spherical and rodlike micelle aggregates formed from a Gemini surfactant: driving forces of micellization and stability of micelles *Langmuir* **32** 7530–40
- [36] Shwann H 1963 Determination of biological impedance *Physical Techniques In Biological Research, VI* (New York: Academic) pp 323–406
- [37] Asami K *et al* 1973 A method for estimating residual inductance in high frequency A.C. measurements *Bull. Inst. Chem. Res. Kyoto Univ.* **51** 231–45
- [38] Hanai T, Imakita T and Koizumi N 1982 Analysis of dielectric relaxations of W/O emulsions in the light of theories of interfacial polarization *Colloid Polym. Sci.* **260** 1029–34
- [39] Bruggeman V D 1935 Berechnung verschiedener physikalischer Konstanten von heterogenen Substanzen. I. Dielektrizitätskonstanten und Leitfähigkeiten der Mischkörper aus isotropen Substanzen *Ann. Phys.* **416** 665–79
- [40] Hanai T 1960 Theory of the dielectric dispersion due to the interfacial polarization and its application to emulsions *Kolloid-Z.* **171** 23–31
- [41] Boyle M 1985 The electrical properties of heterogeneous mixtures containing an oriented spheroidal dispersed phase *Colloid Polym. Sci.* **263** 51–7
- [42] Hanai T, Ishikawa A and Koizumi N 1977 Systematic analysis to determine the dielectric phase parameters from dielectric relaxations caused by diphasic structure of disperse systems *Bull. Inst. Chem. Res. Kyoto Univ.* **55** 376–93
- [43] Folmer B M 2003 Sterol surfactants: from synthesis to applications *Adv. Colloid Interface Sci.* **103** 99–119
- [44] Israelachvili J N, Mitchell D J and Ninham B W 1976 Theory of self-assembly of hydrocarbon amphiphiles into micelles and bilayers *J. Chem. Soc. Faraday Trans. II* **72** 1525–68
- [45] Folmer B M and Nydén M 2008 Structure and dynamics of micelles and cubic phase structures with ethoxylated phytosterol surfactant in water *Langmuir* **24** 6441–6
- [46] Tanford C 1972 Micelle shape and size *J. Phys. Chem.* **76** 3020–4
- [47] Škerjanc J, Ksenija Kogej A and Cerar J 1999 Equilibrium and transport properties of alkyipyridinium bromides *Langmuir* **15** 5023–8
- [48] Fan X and Zhao K 2014 Thermodynamics of micellization of ionic liquids C₆mimBr and orientation dynamics of water for C₆mimBr-water mixtures: a dielectric spectroscopy study *J. Phys. Chem. B* **118** 13729
- [49] Velayutham T S *et al* 2014 Phase sensitive molecular dynamics of self-assembly glycolipid thin films: a dielectric spectroscopy investigation *J. Chem. Phys.* **141** 085101
- [50] Biradar S V, Dhupal R S and Paradka A 2009 Rheological investigation of self-emulsification process *J. Pharm. Pharm. Sci.* **12** 17–31
- [51] Davies M and Swain J 1971 Dielectric studies of configurational changes in cyclohexane and thianthrene structures *Trans. Faraday Soc.* **67** 1637–53
- [52] Smith G *et al* 1996 Dielectric analysis of phosphorylcholine head group mobility in egg lecithin liposomes *Pharm. Res.* **13** 1181–5
- [53] O'Konski C T 1960 Electric properties of macromolecules. V. Theory of ionic polarization in polyelectrolytes *J. Phys. Chem.* **64** 605–19

- [54] Grosse C, Pedrosa S and Shilov V N 2003 Corrected results for the influence of size, ζ potential, and state of motion of dispersed particles on the conductivity of a colloidal suspension *J. Colloid Interface Sci.* **265** 197–201
- [55] Lide D R 2000 *CRC Handbook of Chemistry and Physics* (Boca Raton, FL: CRC Press)
- [56] Fernandez P *et al* 2003 Micelle and solvent relaxation in aqueous sodium dodecylsulfate solutions *ChemPhysChem* **4** 1065–72
- [57] Zhu L and Bratlie K M 2017 Supramolecular assemblies of alkane functionalized polyethylene glycol copolymers for drug delivery *Mater. Sci. Eng. C* **81** 432–42
- [58] Malliaris A, Lang J and Zana R 1986 Micellar aggregation numbers at high surfactant concentration *J. Colloid Interface Sci.* **110** 237–42
- [59] Marianecchi C *et al* 2012 Anti-inflammatory activity of novel ammonium glycyrrhizinate/niosomes delivery system: human and murine models *J. Control. Rel.* **164** 17–25
- [60] Ho M H *et al* 2014 Improving effects of chitosan nanofiber scaffolds on osteoblast proliferation and maturation *Int. J. Nanomed.* **9** 4293–304
- [61] Basiri L, Rajabzadeh G and Bostan A 2017 Physicochemical properties and release behavior of Span 60/Tween 60 niosomes as vehicle for α -tocopherol delivery *LWT Food Sci. Technol.* **84** 471–8